Journal of Engineering Mathematics **46:** 147–163, 2003.
© 2003 *Kluwer Academic Publishers. Printed in the Netherlands.*

Influence of train Mach number on the compression wave generated in a tunnel-entrance hood

M. S. HOWE
Boston University, College of Engineering 110 Cummington Street, Boston MA 02215, U.S.A.
(e-mail: mshowe@bu.edu)

Received 30 July 2002; accepted in revised form 12 November 2002

Abstract. A continuum theory is proposed to study the influence of distributed windows on the compression wave generated by a train entering a tunnel-entrance hood at high Mach numbers. Longer, acoustically noncompact hoods must be used to control the wave-front characteristics at train Mach numbers M between about 0·25 and 0·4. A train entering a fully optimized hood of length ℓ_h produces a compression wave wherein the pressure increases linearly over a wave front of thickness $\sim \ell_h/M$. When M exceeds about 0·2, the interactions of the train nose with windows at opposite ends of the hood become progressively more independent. For a hood whose windows are optimized for low Mach numbers, we show that high-Mach-number operation produces a rapid increase in pressure at the head of the compression-wave front, generated just as the nose enters the hood portal. The pressure rise becomes substantially smoother and close to linear when the nose is within the body of the hood, within the relatively homogeneous environment provided by the distributed windows.

The theory can be extended to permit hood optimization at the high Mach numbers appropriate for magnetically levitated ('Maglev') trains, and to permit the design of 'smart' hoods whose window sizes and distribution can be automatically optimized to suit the speed of an entering train.

Key words: compression wave, high-speed train, Maglev, micro-pressure wave, tunnel-entrance hood

1. Introduction

The pressure rise Δp across the front of the compression wave generated in a tunnel of cross-sectional area $\mathcal{A}$ ahead of an entering train of cross-section $\mathcal{A}_0$ is given approximately by

$$\Delta p \sim \frac{\rho_o U^2}{(1-M^2)}\frac{\mathcal{A}_0}{\mathcal{A}}\left(1+\frac{\mathcal{A}_0}{\mathcal{A}}\right) \tag{1.1}$$

provided the 'blockage' $\mathcal{A}_0/\mathcal{A}$ is less than about 0·25, where ρ_o is the mean air density, U the train speed, and $M = U/c_o$ is the train Mach number (c_o = speed of sound in air) [1–7]; Δp can exceed 2 or 3% of the atmospheric pressure at speeds U of 250 kph (150 mph) or more.

The wave front thickness $\sim R/M$, where R is the radius of the equivalent semi-circular tunnel of the same cross-sectional area, and the front advances into the tunnel at the speed of sound. However, acoustic nonlinearity (producing wave front steepening) can result in a significant reduction in wave thickness in a long tunnel fitted with 'acoustically smooth' concrete slab tracks . This can greatly increase the strength of the acoustic pulse – the *micro-pressure wave* – radiated from the far end of the tunnel when the compression wave arrives, because the amplitude of the pulse is proportional to the steepness of the incident compression wave. The micro-pressure wave can excite annoying structural 'rattles' and vibrations in buildings near the tunnel exit – it is one of the most important impediments to further increases in train speed.

(a)

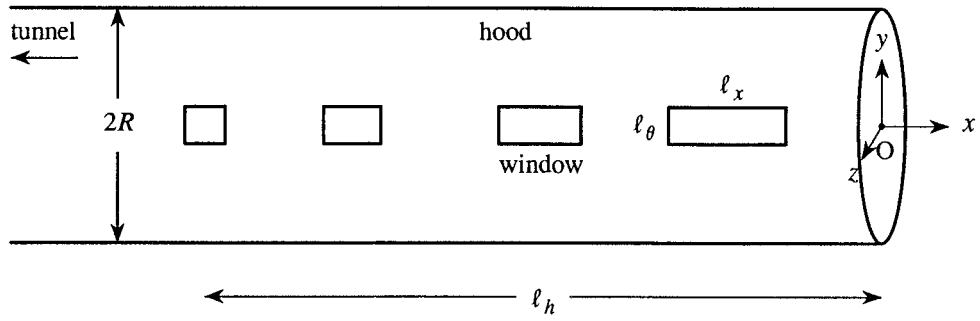

(b)

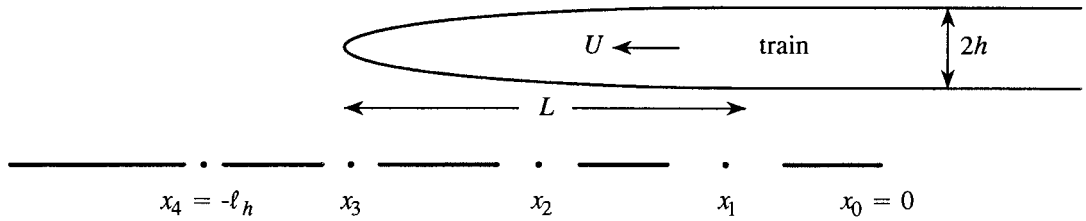

Figure 1. (a) Schematic of the circular cylindrical tunnel of radius R fitted with a hood of length ℓ_h when there are $N = 4$ rectangular windows. The geometric centre of the nth window is at $x = x_n$, $y = 0$, $z = R$. (b) Characteristic dimensions of an axisymmetric train entering the hood at speed U along the centreline of the tunnel.

Nonlinear steepening tends to be inhibited if the initial wave thickness is sufficiently large, and effective suppression of the micro-pressure wave can often be achieved by installing a 'hood' ahead of the tunnel entrance. They have been used in Japan since 1977. The hood consists of a thin-walled tunnel extension that increases the initial compression wave thickness by permitting the release of high-pressure air in front of an entering train through 'windows' strategically placed along the hood walls [6, 8, 9] (Figure 1 shows schematically a hood attached to the entrance of a circular cylindrical tunnel frequently used in model scale experiments). In an optimally designed hood of length ℓ_h, the train produces a compression-wave front initially of thickness $\sim \ell_h/M$ across which the pressure rises *linearly*. In practice the hood length ℓ_h depends on tunnel length and the maximum expected train speed, and may be assumed to be prescribed for the purpose of optimizing hood design. It is feasible to use model scale tests to determine the appropriate window size and spacing for the relatively short hoods ($\ell_h \sim 3R$) required for conventional high-speed operations ($M \leq 0{\cdot}2$). But much longer hoods (say $\ell_h \approx 10R$, [10]) will be necessary at the projected higher speeds of newer trains, involving M as large as 0·4 for 'Maglev' types (when (1.1) implies that $\Delta p \sim 6\%$ atmospheric pressure).

It then becomes impracticable to base hood design entirely on *ad hoc* experimentation. The author [11] has developed an approximate analytical scheme for determining the optimal spacing and sizing of windows in a long hood that is strictly applicable when the wave thickness $\sim \ell_h/M$ can be regarded as very much larger than the hood length ℓ_h, that is, when the hood length ℓ_h is 'compact' – short compared to the wavelengths of the principal acoustic pressure transients generated by the train. This approximation is valid at the lower Mach numbers of conventional trains ($M < 0{\cdot}2$), but the increased importance of compressible flow effects within the hood at higher values of M can be expected to produce significant departures of the initial compression-wave profile from the optimal linear form.

In this paper the earlier theory [11] for the design of an optimal compact hood is developed further to examine high-Mach-number effects. The compact design is expected to be adequate for Mach numbers at least as large as $M = 0{\cdot}2$. The objective here is to take such an optimally designed compact hood, with window spacing and sizing prescribed for optimum operation at low Mach number, and examine how the compression-wave front varies from the ideal linear profile as the Mach number is increased. Model scale experiments [12] suggest that the theory is applicable when the blockage $\mathcal{A}_0/\mathcal{A} \leq 0{\cdot}2$; this condition is satisfied in all anticipated applications at full scale.

The analytical theory of compression-wave formation is reviewed in Section 2; the formal analytical representation of the wave in terms of a Green's function is discussed in Section 3 for a circular cylindrical hood with an arbitrary prescribed distribution of windows. The compact approximation is derived in Section 4, and extended in Section 5 to include compressible effects within the hood. Numerical results are presented that illustrate the progressive degradation of the compression wave front profile from its optimal linear form with increasing values of the train Mach number. Explicit results are discussed only for a tunnel and hood of the same circular cylindrical cross-section, of the type used in model scale experimental studies [3, 5–8, 11], although the method is easily modified to deal with more general geometries.

2. Representation of the compression wave

Consider a circular cylindrical tunnel of radius R and cross-sectional area $\mathcal{A} = \pi R^2$ fitted with a cylindrical hood of the same cross-section having N windows distributed along the hood parallel to the tunnel axis (Figure 1). Take coordinate axes $\mathbf{x} = (x, y, z)$ with the origin O on the cylinder axis in the entrance plane of the hood, with the x-axis coaxial with the cylinder and directed out of the tunnel. To fix ideas let the centroid of the nth window be at $x = x_n,\ y = 0,\ z = R\ (1 \leq n \leq N)$, $-\ell_h = x_N < x_{N-1} < \cdots < x_1 < 0$, where ℓ_h is the hood length. The window at x_n may be regarded as curvilinear rectangular with length ℓ_x parallel to the cylinder axis and azimuthal length ℓ_θ.

In a typical experiment an axisymmetric 'train' of maximum radius h is projected at high speed into the tunnel from $x > 0$, guided by a steel wire tightly stretched along the tunnel axis and threaded through a smooth cylindrical bore hole along the train axis. We shall present numerical results for this case, but our formulae will also apply to situations where the 'track' does not coincide with the tunnel axis. The compression wave is generated as the front of the train passes through the hood. To calculate the initial wave front profile the tunnel may be assumed to extend to $x = -\infty$, and the train regarded as semi-infinite, with uniform circular cross-sectional area $\mathcal{A}_0 = \pi h^2$ to the rear of the 'nose' of length L shown in the figure.

The initial pressure rise across the compression wave front depends on train Mach number M and on the blockage $\mathcal{A}_o/\mathcal{A}$. The train can be represented by a set of monopole and dipole sources translating with the train that account for the displacement of air by the train and the pressure drag over the nose. The characteristics of the compression wave front profile are governed by the interaction of these sources with the hood portal and windows [5, 6, 8, 9, 12–14]. The pressure continues to rise slowly behind the wave front because of the action of additional 'vortex sources' in the boundary layers on the train and tunnel walls and in the exit flows from the portal and windows [15]. The contributions of these sources to the formation of the compression wave is of secondary importance, and they are ignored in the present discussion.

When the train enters the tunnel from $x > 0$ along the tunnel-axis at constant speed U, and the blockage $\mathcal{A}_o/\mathcal{A} \leq 0{\cdot}2$, it is found to a good approximation that the monopole and dipole sources may be taken to lie along the axis of the train (a 'slender body approximation') [13]. The compression wave is then determined by the solution of

$$\left(\frac{1}{c_o^2}\frac{\partial^2}{\partial t^2} - \nabla^2\right) B = U\left(1 + \frac{\mathcal{A}_o}{\mathcal{A}}\right)\frac{\partial}{\partial t}\left(\frac{\partial \mathcal{A}_T}{\partial x}(x + Ut)\delta(y)\delta(z)\right), \tag{2.1}$$

where

$$B = \frac{p}{\rho_o} + \frac{1}{2}v^2 \tag{2.2}$$

is the total enthalpy, and p and $\mathbf{v}$ are, respectively, the perturbation air pressure and the flow velocity. The front of the train is assumed to cross the entrance plane of the hood ($x = 0$) at time $t = 0$, and $\mathcal{A}_T(s)$ is the cross-sectional area of the train at distance s from the tip of the nose. The source term evidently vanishes except in the nose region, where the train cross-section is changing.

In the tunnel far ahead of the train the compression wave produces a small amplitude disturbance, and the pressure rise can be determined from the solution of (2.1) by means of the linearized approximation

$$p \approx \rho_o B, \quad x \to -\infty. \tag{2.3}$$

This is strictly valid only in the initial stages of the formation of the wave front, prior to any nonlinear steepening. A knowledge of this solution, however, is sufficient for studies of optimal hood design.

Equation (2.1) can be solved in terms of a Green's function $G(\mathbf{x}, \mathbf{x}', t - \tau)$, determined by the solution of

$$\left(\frac{1}{c_o^2}\frac{\partial^2}{\partial t^2} - \nabla^2\right) G = \delta(\mathbf{x} - \mathbf{x}')\delta(t - \tau), \quad G = 0 \ \text{ for } t < \tau, \tag{2.4}$$

where

$$\frac{\partial G}{\partial x_n} = 0 \quad \text{on the interior and exterior walls of the tunnel and hood,} \tag{2.5}$$

and where x_n is a local coordinate in the normal direction from the wall. When the vorticity $\boldsymbol{\omega} = \mathbf{0}$, the air velocity $\mathbf{v} = \nabla\phi$ where ϕ and the total enthalpy B satisfy $B = -\partial\phi/\partial t$, [13], so that (2.5) corresponds to the usual rigid wall boundary condition of potential theory.

Approximate functional forms of G are discussed later in this paper. However, in all cases our approximations will involve the assumption that the tunnel diameter and window dimensions are small compared to the characteristic compression wave thickness. This turns out to be equivalent to expanding the solution to *first order* in the Mach number M; to this order the solution includes a correct representation of *phase* differences between interactions of different windows with the train nose, but the predicted *overall* wave amplitude is too small by a factor $1/(1-M^2)$, [12, 14]. We shall compensate for this at the outset by replacing the source term in (2.1) by

$$\frac{U}{(1-M^2)}\left(1+\frac{\mathcal{A}_0}{\mathcal{A}}\right)\frac{\partial}{\partial t}\left(\frac{\partial \mathcal{A}_T}{\partial x}(x+Ut)\delta(y)\delta(z)\right). \tag{2.6}$$

This correction represents a mean (as opposed to transient) effect of compressibility. It has been validated in [12] by comparison of predictions for flanged and flared tunnel portals with experiment, and in [14] by consideration of the exact analytical solution for a circular cylindrical tunnel with no windows.

Then, Green's function and Equations (2.1), (2.3), with the modification (2.6), yield

$$\begin{aligned} p &\approx \frac{\rho_o U}{(1-M^2)}\left(1+\frac{\mathcal{A}_0}{\mathcal{A}}\right)\frac{\partial}{\partial t}\int_{-\infty}^{\infty}\frac{\partial \mathcal{A}_T}{\partial x'}(x'+U\tau)G(\mathbf{x},x',0,0,t-\tau)\mathrm{d}x'\mathrm{d}\tau \\ &= \frac{-\rho_o U^2}{(1-M^2)}\left(1+\frac{\mathcal{A}_0}{\mathcal{A}}\right)\int_{-\infty}^{\infty}\frac{\partial \mathcal{A}_T}{\partial x'}(x'+U\tau)\frac{\partial G}{\partial x'}(\mathbf{x},x',0,0,t-\tau)\mathrm{d}x'\mathrm{d}\tau, \quad x\to-\infty, \end{aligned} \tag{2.7}$$

where the second line is obtained by differentiating with respect to time under the integral sign and integrating by parts first with respect to τ and then x' (noting that $\partial \mathcal{A}_T/\partial x'$ vanishes at $x'=\pm\infty$).

But the compression wave is formed progressively as the train nose interacts first with the hood portal and then with the windows, and in numerical work it is usually convenient to isolate these interactions by using (2.7) to calculate the *pressure gradient* $\partial p/\partial t$ (instead of p), because this vanishes except in the vicinity of the compression wave front. In this case we have (after integration by parts, as above)

$$\frac{\partial p}{\partial t} \approx \frac{\rho_o U^3}{(1-M^2)}\left(1+\frac{\mathcal{A}_0}{\mathcal{A}}\right)\int_{-\infty}^{\infty}\frac{\partial \mathcal{A}_T}{\partial x'}(x'+U\tau)\frac{\partial^2 G}{\partial x'^2}(\mathbf{x},x',0,0,t-\tau)\mathrm{d}x'\mathrm{d}\tau, \quad x\to-\infty. \tag{2.8}$$

When this has been evaluated the pressure p is computed from

$$p=\int_{-\infty}^{t}\frac{\partial p}{\partial t'}\,\mathrm{d}t'. \tag{2.9}$$

3. Green's function

3.1. The diffraction problem

The solution (2.8) for the compression wave pressure gradient is strictly applicable in the tunnel at large distances from the hood. The integrand is significantly different from zero only during the interval in which the train nose crosses the hood, so that the source point $\mathbf{x}'$ of Green's function $G(\mathbf{x},\mathbf{x}',t-\tau)$ may be regarded as confined to the vicinity of the hood. To determine G we set

$$G(\mathbf{x},\mathbf{x}',t-\tau)=-\frac{1}{2\pi}\int_{-\infty}^{\infty}\bar{G}(\mathbf{x},\mathbf{x}',\omega)\mathrm{e}^{-\mathrm{i}\omega(t-\tau)}\,\mathrm{d}\omega. \tag{3.1}$$

Then $\bar{G}$ satisfies

$$(\nabla^2+\kappa_o^2)\bar{G}=\delta(\mathbf{x}-\mathbf{x}'),\quad \text{where } \kappa_o=\frac{\omega}{c_o}. \tag{3.2}$$

We shall solve this in the usual way by application of the reciprocal theorem [19, p. 145] that $\bar{G}(\mathbf{x},\mathbf{x}',\omega)\equiv\bar{G}(\mathbf{x}',\mathbf{x},\omega)$. The point source in (3.2) is regarded as placed at $\mathbf{x}$ within the tunnel (where $x\to-\infty$) and the solution is sought as a function of $\mathbf{x}'$ within and near the hood. This greatly simplifies the calculations because the characteristic wavelength of the compression wave front is much larger than the tunnel radius R, so that its principal Fourier components in (3.1) are plane waves propagating parallel to the tunnel axis. The solution of (3.2) must therefore be found only for values of $\kappa_o R$ smaller than about 3·82 in magnitude [16, p. 111], corresponding to the axially propagating components of the compression wave.

When this condition is satisfied the reciprocal point source at $\mathbf{x}$ ($x\to-\infty$) generates a disturbance that propagates towards the hood (as a function of x') in the form of the plane wave

$$\bar{G}_{\mathrm{I}}=\frac{\mathrm{e}^{\mathrm{i}\kappa_o(x'-x)}}{2\mathrm{i}\kappa_o\mathcal{A}}. \tag{3.3}$$

The functional form of $\bar{G}(\mathbf{x}',\mathbf{x},\omega)$ is now determined by considering the 'diffraction' of $\bar{G}_{\mathrm{I}}$ by the hood windows and portal.

To do this we write, for all points in the hood and in the tunnel close to the hood,

$$\bar{G}=\frac{\mathrm{e}^{-\mathrm{i}\kappa_o x}}{\mathcal{A}}\varphi(\mathbf{x}',\kappa_o),\quad x'<0, \tag{3.4}$$

where within the tunnel

$$\varphi=\frac{1}{2\mathrm{i}\kappa_o}\left\{\mathrm{e}^{\mathrm{i}\kappa_o x'}+\mathcal{R}\mathrm{e}^{-\mathrm{i}\kappa_o x'}\right\}. \tag{3.5}$$

The second formula is applicable when $\mathbf{x}'$ is to the 'left' of the innermost hood window in Figure 1, say for $x'<-\ell_h-2R$: the first term in the brace brackets corresponds to the incident plane wave (3.3); $\mathcal{R}$ is a reflection coefficient that accounts for the interaction of the incident wave with the hood and portal.

When $\varphi(\mathbf{x}',\kappa_o)$ has been determined (3.1) supplies

$$G(\mathbf{x},\mathbf{x}',t-\tau)=-\frac{1}{2\pi\mathcal{A}}\int_{-\infty}^{\infty}\varphi(\mathbf{x}',\kappa_o)\mathrm{e}^{-\mathrm{i}\omega(t-\tau+x/c_o)}\,\mathrm{d}\omega,\quad x\to-\infty, \tag{3.6}$$

and the formulae (2.7) and (2.8) for the compression wave pressure and pressure gradient assume the forms

$$p\approx\frac{\rho_o U^2}{2\pi(1-M^2)\mathcal{A}}\left(1+\frac{\mathcal{A}_{\mathrm{o}}}{\mathcal{A}}\right)\int_{-\infty}^{\infty}\frac{\partial\mathcal{A}_{\mathrm{T}}}{\partial x'}(x'+U\tau)\frac{\partial\varphi}{\partial x'}(x',0,0,\kappa_o)\mathrm{e}^{-\mathrm{i}\omega(t-\tau+x/c_o)}\mathrm{d}x'\mathrm{d}\tau\mathrm{d}\omega, \tag{3.7}$$

$$\frac{\partial p}{\partial t}\approx\frac{-\rho_o U^3}{2\pi(1-M^2)\mathcal{A}}\left(1+\frac{\mathcal{A}_{\mathrm{o}}}{\mathcal{A}}\right)\int_{-\infty}^{\infty}\frac{\partial\mathcal{A}_{\mathrm{T}}}{\partial x'}(x'+U\tau)\frac{\partial^2\varphi}{\partial x'^2}(x',0,0,\kappa_o)\mathrm{e}^{-\mathrm{i}\omega(t-\tau+x/c_o)}\mathrm{d}x'\mathrm{d}\tau\mathrm{d}\omega, \tag{3.8}$$

as $x \to -\infty$.

In an optimally designed hood the function φ must be chosen to make the pressure increase smoothly and 'linearly' across a compression wave front of thickness $\sim \ell_h/M$. But the functional form of φ depends on the distribution of the windows, and cannot yield a perfectly linear wave profile when the windows are distributed discretely (as opposed to continuously) along the hood. Similarly, details of the compression-wave front also depend on the shape of the train nose, determined by $\mathcal{A}_{\mathrm{T}}(x)$; this dependence will be weak, however, if $\mathcal{A}_{\mathrm{o}}/\mathcal{A}$ is small, when in a first approximation the distributed source over the nose region of the train may be regarded as equivalent to a source concentrated on the train axis at the centroid of the nose.

For these reasons it is sufficient to formulate the hood design problem in terms of the simplified forms assumed by equations (3.7), (3.8) for a 'snub nosed' train, whose nose length $L \to 0$, and for which

$$\frac{\partial \mathcal{A}_{\mathrm{T}}}{\partial x'}(x' + Ut) \to \mathcal{A}_{\mathrm{o}}\delta(x' + Ut). \tag{3.9}$$

We note here for future reference the particular reduced forms of (3.7) and (3.8) in this case:

$$p \approx \frac{\rho_o U^2}{2\pi(1-M^2)}\frac{\mathcal{A}_{\mathrm{o}}}{\mathcal{A}}\left(1+\frac{\mathcal{A}_{\mathrm{o}}}{\mathcal{A}}\right)\int_{-\infty}^{\infty}\frac{\partial\varphi}{\partial x'}(-U\tau,0,0,\kappa_o)\mathrm{e}^{-\mathrm{i}\omega(t-\tau+x/c_o)}\mathrm{d}\tau\,\mathrm{d}\omega, \quad x \to -\infty, \tag{3.10}$$

and

$$\frac{\partial p}{\partial t} \approx \frac{-\rho_o U^3}{2\pi(1-M^2)}\frac{\mathcal{A}_{\mathrm{o}}}{\mathcal{A}}\left(1+\frac{\mathcal{A}_{\mathrm{o}}}{\mathcal{A}}\right)\int_{-\infty}^{\infty}\frac{\partial^2\varphi}{\partial x'^2}(-U\tau,0,0,\kappa_o)\mathrm{e}^{-\mathrm{i}\omega(t-\tau+x/c_o)}\mathrm{d}\tau\,\mathrm{d}\omega, \; x \to -\infty. \tag{3.11}$$

3.2. Determination of φ

The functional form of φ within the hood is governed by the Helmholtz equation

$$(\nabla'^2 + \kappa_o^2)\varphi = 0, \tag{3.12}$$

where the Laplacian ∇'^2 is with respect to the dependence of φ on $\mathbf{x}'$. The solution must satisfy appropriate boundary conditions at the windows and at the hood portal, and cannot normally be obtained in analytic form. Analytical approximations for special cases in which the windows are replaced by a continuous distribution of small perforations, or when there is only one window, have been investigated in [15, 17, 18]. The procedure we shall adopt here, however, is a development of the approximation proposed in [11] for a compact hood, where the variation of φ along the track of the train is determined in two stages I and II. In the first stage the individual windows are ignored, and $\varphi = \varphi_{\mathrm{I}}$ is calculated by taking account merely of their collective, spatially averaged contribution to the solution; this averaged solution depends only on axial location within the hood, $\varphi_{\mathrm{I}} = \varphi_{\mathrm{I}}(x', \kappa_o)$, and is used to determine the effective 'source strength' of each window. When the size and shape of the nth window are known the volume flux $q_n(\kappa_o)$ through the window *directed out of the hood* can be found from Rayleigh's formula [19, pp. 172–180]

$$q_n(\kappa_0) = -K_n\varphi_{\mathrm{I}}(x_n, \kappa_o) \tag{3.13}$$

where K_n is the *conductivity* of the window. In writing down this formula it is assumed that the magnitude of the analytic continuation of $\varphi_{\rm I}(x', \kappa_o)$ to the free space region *outside* the hood is negligibly small, so that the mean potential rise along a curve passing from x_n on the tunnel axis out through the window is just equal to $-\varphi_{\rm I}(x_n, \kappa_o)$. Similarly, it is usually permissible to assume that, even when the hood as a whole ceases to be compact, each window (of dimensions $\ell_x \times \ell_\theta$) remains compact, in which case the conductivity K_n will be independent of κ_o. When $q_n(\kappa_0)$ is known for each window a second approximation for φ can then be derived (in the manner to be described below) by introducing the exact representations in the tunnel and hood of the potential fields of the window sources.

The method used in [11] for stage I of the calculation was based on a one-dimensional, step function approximation to the variation of $\partial\varphi_{\rm I}/\partial x'$ within the hood, the step changes occurring across the points $x' = x_n$ marking the centroids of successive windows. In order to extend this procedure to include the influence of compressibility, however, it is more convenient to use a continuum theory, by introducing on the right of Equation (3.12) a 'smeared out' representation of the influence of the windows. As viewed from the tunnel axis, each window behaves as a sink (a source of strength $-q_n(\kappa_0)$) of air perturbed by the incident wave (3.3). These are approximated in the first stage of the calculation by replacing the discrete distribution of sinks by a continuous *line sink* of variable strength $Q(x', \kappa_o)$ extending over the length $-\ell_h < x' < 0$ of the hood. Thus, the one dimensional equation satisfied by $\varphi_{\rm I}$ in the hood is

$$\frac{\partial^2\varphi_{\rm I}}{\partial x'^2} + \kappa_o^2\varphi_{\rm I} = -Q(x', \kappa_o), \quad -\ell_h < x' < 0, \tag{3.14}$$

where $Q(x', \kappa_o)$ remains to be determined.

When $Q(x', \kappa_o)$ is known, Equation (3.14) is to be solved subject to conditions to be imposed at the ends of the hood. At the inner end ($x' = -\ell_h$) we require that the values of $\varphi_{\rm I}$ and $\partial\varphi_{\rm I}/\partial x'$ should equal those determined by the one-dimensional plane waves of (3.5), so that

$$\left.\begin{aligned} \varphi_{\rm I} &= \frac{1}{2{\rm i}\kappa_o}\left\{{\rm e}^{-{\rm i}\kappa_o\ell_h} + \mathcal{R}{\rm e}^{{\rm i}\kappa_o\ell_h}\right\} \\ \frac{\partial\varphi_{\rm I}}{\partial x'} &= \frac{1}{2}\left\{{\rm e}^{-{\rm i}\kappa_o\ell_h} - \mathcal{R}{\rm e}^{{\rm i}\kappa_o\ell_h}\right\} \end{aligned}\right\} \text{ at } x' = -\ell_h. \tag{3.15}$$

In other words, $\varphi_{\rm I}$ must satisfy

$$\frac{\partial\varphi_{\rm I}}{\partial x'} + {\rm i}\kappa_o\varphi_{\rm I} = {\rm e}^{-{\rm i}\kappa_o\ell_h} \quad \text{at } x' = -\ell_h. \tag{3.16}$$

At the hood portal ($x' = 0$) we require $\varphi_{\rm I}$ to behave in the same way as the potential of uniform flow from a circular cylindrical duct. This should be an adequate approximation in practice provided that the centroid of the first window (at $x' = x_1$) is at least about one tunnel diameter from the entrance plane of the hood. Because the motion in the portal differs negligibly from that of an incompressible fluid, this means that [11, 13]

$$\varphi_{\rm I} = -V\ell', \quad \frac{\partial\varphi_{\rm I}}{\partial x'} = V, \quad \text{as } x' \to -0, \tag{3.17}$$

where $\ell' \approx 0{\cdot}61R$ is the 'end correction' of an unflanged duct of radius R [16, pp. 114–115, 19, pp. 487–491], and $V = V(\kappa_o)$ is the mean flow speed $\partial\varphi_{\rm I}/\partial x'$ at the portal, whose value is

initially unknown. When φ_{I} has been determined within the hood to satisfy these conditions, its definition may be extended to the x-axis outside the hood portal, where it may be regarded as matched on to the velocity potential describing flow from a circular cylindrical duct. In this exterior domain φ_{I} will decrease rapidly with distance from the portal, and may to a sufficient approximation be represented by the potential for *incompressible flow*.

4. The compact hood

4.1. Stage I approximation

Consider first the hood characteristics at sufficiently small train Mach number M that the hood length ℓ_h is compact. We shall suppose the hood is optimized for such operations, and determine subsequently the influence of finite Mach number on this optimal behaviour. The neglect of compressible effects within the hood implies that $\varphi_{\mathrm{I}} \equiv \varphi_{\mathrm{I}}(x', 0)$ does not depend on the acoustic wavenumber κ_o. Then Equation (3.14) becomes

$$\frac{\partial^2 \varphi_{\mathrm{I}}}{\partial x'^2}(x', 0) = -Q(x', 0), \quad -\ell_h < x' < 0, \tag{4.1}$$

and conditions (3.16), (3.17) reduce to

$$\begin{aligned} \frac{\partial \varphi_{\mathrm{I}}}{\partial x'}(x', 0) \;&=\; 1 \;\text{ at } x' = -\ell_h; \\ \varphi_{\mathrm{I}}(x', 0) \;&=\; -V_0 \ell', \;\; \frac{\partial \varphi_{\mathrm{I}}}{\partial x'}(x', 0) \;=\; V_0 \;\text{ as } x' \to -0. \end{aligned} \tag{4.2}$$

In these conditions V_0 is a positive constant that determines the volume flux from the portal at mean velocity $\partial \varphi_{\mathrm{I}}/\partial x' = V_0$; it lies in the range $0 < V_0 < 1$, because the outflow into the sink (through the 'windows') implies that the flux from the portal cannot exceed that in the tunnel.

For an optimally designed hood the pressure increases *linearly* across a compression wave front of thickness $\sim \ell_h/M$. This condition is used to determine the sink distribution function $Q(x', 0)$ by consideration of the snub nosed train (3.9). When φ is replaced by $\varphi_{\mathrm{I}}(x', 0)$ in formula (3.10) defining the compression wave pressure in this case, the frequency ω occurs only in the exponential factor, whose infinite integral with respect to ω is equal to

$$2\pi\,\delta\left(t - \tau + \frac{x}{c_o}\right)$$

Hence, for the snub-nosed train

$$p \approx \frac{\rho_{\mathrm{o}} U^2}{(1 - M^2)} \frac{\mathcal{A}_{\mathrm{o}}}{\mathcal{A}} \left(1 + \frac{\mathcal{A}_{\mathrm{o}}}{\mathcal{A}}\right) \frac{\partial \varphi_{\mathrm{I}}}{\partial x'} \left(-U[t], 0\right), \quad x \to -\infty, \;\text{ where } \; [t] = t + \frac{x}{c_o}. \tag{4.3}$$

Conditions (4.2) imply that $\partial \varphi_{\mathrm{I}}/\partial x'$ in this formula increases from 0 to 1 as the retarded time $[t]$ increases from a value marginally less than zero to $U[t] > \ell_h$. The hood will therefore behave optimally provided

$$\frac{\partial \varphi_{\mathrm{I}}}{\partial x'}(x', 0) \;\text{ decreases linearly as } x' \text{ increases over } \; -\ell_h < x' < 0.$$

For this to be possible the sink strength Q in (4.1) must be constant. Then

$$\varphi_{\rm I}(x',0) = V_0(x'-\ell') - \frac{(1-V_0)x'^2}{2\ell_h}, \quad -\ell_h < x' < 0, \quad \text{and} \quad Q(x',0) = \frac{1-V_0}{\ell_h}. \quad (4.4)$$

4.2. STAGE II APPROXIMATION

In stage II of the calculation $\varphi_{\rm I}(x',0)$ is used to determine the window dimensions and the contribution of each window to the compression wave profile.

The volume flux from the nth window (whose centroid is at $x' = x_n$) when $\kappa_o = 0$ is $q_n(0)$ $(1 \le n \le N)$. This will be set to equal the net change in the axial volume flux determined by $\varphi_{\rm I}(x',0)$ within the hood between $x' = x_n$ and $x' = x_{n-1}$. Then

$$q_n(0) = \mathcal{A}\left\{\frac{\partial\varphi_{\rm I}}{\partial x'}(x_n,0) - \frac{\partial\varphi_{\rm I}}{\partial x'}(x_{n-1},0)\right\} = \frac{\mathcal{A}(1-V_0)}{\ell_h}(x_{n-1}-x_n), \ n = 1,\ 2,\ \ldots,\ N, \quad (4.5)$$

where $x_0 = 0$ (as in Figure 1).

Consider next the use of these results to calculate the pressure gradient $\partial p/\partial t$ from (3.8), or for the snub-nosed train using (3.11) for a compact hood with a discrete distribution of N windows. In our continuum model $\partial^2\varphi_{\rm I}/\partial x'^2$ is constant within the hood, but the true second derivative $\partial^2\varphi/\partial x'^2$ is actually significantly different from zero only in the immediate vicinity of a window and at the hood portal. We shall therefore assume that in the case of a distribution of discrete windows, the contribution to $\varphi(\mathbf{x},0)$ of the potential flux $q_n(0)$ from the nth window can be approximated by the incompressible velocity potential

$$\frac{q_n(0)}{\mathcal{A}}\varphi_n(\mathbf{x}),$$

say, produced by a point *sink* of strength $q_n(0)$ at the centroid $(x_n, 0, R)$ of the window. The justification of this hypothesis rests entirely on the resulting predictions of the compression wave profile, to be discussed below.

Introduce cylindrical polar coordinates (r,θ,x) defined such that $(z,y) = r(\cos\theta,\sin\theta)$. Then routine calculation yields the formula

$$R\frac{\partial^2\varphi_n}{\partial x^2}(r,\theta,x) = \frac{-1}{\pi}\sum_{m=0}^{\infty}\int_0^\infty \frac{\sigma_m\cos(m\theta)\lambda}{{\rm I}_{m+1}(\lambda)+{\rm I}_{m-1}(\lambda)}{\rm I}_m\left(\frac{\lambda r}{R}\right)\cos\left(\frac{\lambda(x-x_n)}{R}\right)\,{\rm d}\lambda, \ r < R, \quad (4.6)$$

where ${\rm I}_\nu$ is a modified Bessel function [20, Section 9.6], and $\sigma_0 = 1,\ \sigma_m = 2$ $(m \ge 1)$.

A similar integral expression can be derived [13] for the velocity potential $V_0\varphi_0(\mathbf{x})$, say, representing potential flow from the the hood portal, namely

$$\begin{aligned} R\frac{\partial^2\varphi_0}{\partial x^2}(r,\theta,x) &= -\frac{1}{2\pi}\int_0^\infty \lambda{\rm I}_0\left(\frac{\lambda r}{R}\right)\left(\frac{2{\rm K}_1(\lambda)}{{\rm I}_1(\lambda)}\right)^{\frac12}\cos\left\{\lambda\left(\frac{x}{R}+\mathcal{Z}(\lambda)\right)\right\}{\rm d}\lambda, \quad r < R, \\ \mathcal{Z}(\lambda) &= \frac{1}{\pi}\int_0^\infty \log\left(\frac{{\rm K}_1(\mu){\rm I}_1(\mu)}{{\rm K}_1(\lambda){\rm I}_1(\lambda)}\right)\frac{{\rm d}\mu}{\mu^2-\lambda^2}. \end{aligned} \quad (4.7)$$

where ${\rm K}_1$ is a modified Bessel function [20, Section 9.6].

Hence, our corrected estimate of $\partial^2\varphi/\partial x^2$ for use in (3.8) and (3.11) is

$$\frac{\partial^2\varphi}{\partial x^2}(\mathbf{x},0) = \sum_{n=1}^{N}\frac{q_n(0)}{\mathcal{A}}\frac{\partial^2\varphi_n}{\partial x^2}(r,\theta,x) + V_0\frac{\partial^2\varphi_0}{\partial x^2}(r,\theta,x), \quad r < R. \quad (4.8)$$

This is non-zero only within the hood in the vicinities of the windows, and at the hood portal. The monopole strengths q_n are given in terms of V_0 and the window coordinates by (4.5); the coefficient V_0 remains to be specified.

4.3. WINDOW DIMENSIONS

The size of the nth window is estimated from the formula

$$K_n = \frac{-q_n(0)}{\varphi_1(x_n, 0)}, \tag{4.9}$$

where K_n is the conductivity of the window introduced above in (3.13). According to Rayleigh [19, pp. 180–182], when the area $\mathcal{A}_n$ of the nth window is much smaller than the cross-section $\mathcal{A}$ of the hood and the hood wall has thickness ℓ_w

$$\frac{1}{K_n} \approx \sqrt{\frac{\pi}{4\mathcal{A}_n}} + \frac{\ell_w}{\mathcal{A}_n}. \tag{4.10}$$

Therefore, using the formulae (4.4) and (4.5), we find

$$\mathcal{A}_n \approx \frac{\pi K_n^2}{16}\left(1 + \sqrt{1 + \frac{16\ell_w}{\pi K_n}}\right)^2,$$

where

$$K_n = \frac{\mathcal{A}(x_{n-1} - x_n)}{x_n^2/2 - V_0\ell_h(x_n - \ell')/(1 - V_0)}. \tag{4.11}$$

4.4. EVENLY SPACED WINDOWS

We shall give numerical illustrations of the theory for evenly spaced windows, when, from (4.5), $x_n = -n\ell_h/N,\ 0 \le n \le N$, and

$$q_n(0) = \frac{\mathcal{A}(1 - V_0)}{N},\ 1 \le n \le N. \tag{4.12}$$

Then

$$K_n = \frac{2N\mathcal{A}}{n^2\ell_h + 2NV_0(n\ell_h + N\ell')/(1 - V_0)},\ 1 \le n \le N; \tag{4.13}$$

$$\frac{\partial^2\varphi}{\partial x^2}(r, \theta, x, 0) = \frac{(1 - V_0)}{N}\sum_{n=1}^{N}\frac{\partial^2\varphi_n}{\partial x^2}(r, \theta, x) + V_0\frac{\partial^2\varphi_0}{\partial x^2}(r, \theta, x),\quad r < R. \tag{4.14}$$

The optimal value of the nondimensional velocity V_0 is the same as for the step-function model for $\varphi(\mathbf{x}, 0)$ discussed in [11], namely

$$V_0 = \frac{1}{1 + 0{\cdot}72N}. \tag{4.15}$$

This value ensures that as x increases from $x = -\ell_h$ to some value of x just beyond the hood portal, the decrease in $\partial\varphi/\partial x$ from 1 to 0 is approximately linear. Such a variation is not actually possible when the hood has a finite number of windows, but can be closely attained if V_0 is chosen to make the mean value of $R\partial^2\varphi/\partial x^2$ roughly constant. In general, the value of V_0 will depend somewhat on the position of the train track inside the tunnel. We shall consider only the experimental case where the train travels along the tunnel axis ($r = 0$).

For each n and fixed values of r and θ, it is clear from (4.6) that $R\partial^2\varphi_n/\partial x^2$ is an even function of $x - x_n$; it exhibits a single maximum negative peak value at $x = x_n$. On the tunnel axis this maximum value is approximately equal to $-0{\cdot}89$. When the windows are evenly spaced the series on the right of (4.14) therefore defines a function of x that varies periodically from window to window within the hood, assuming equal negative maxima of $-0{\cdot}89(1 - V_0)/NR$ at each window, and tending rapidly to zero outside the hood portal in $x > 0$. The final term $V_0\partial^2\varphi_0/\partial x^2$ on the right of (4.14) is negative and non-zero only near $x = 0$, where it attains a negative maximum value of $-0{\cdot}64V_0/R$. The *average* negative value of $\partial^2\varphi(\mathbf{x}, 0)/\partial x^2$ will be approximately constant within the hood and in the immediate neighbourhood of the hood portal if all of the peak negative values are taken to be equal, and this condition leads to (4.15).

Figure 2 illustrates for three different values of V_0 the variations of $R\partial^2\varphi(\mathbf{x}, 0)/\partial x^2$ given by (4.14) and the wavy yet linear variations of $\partial\varphi(\mathbf{x}, 0)/\partial x$ (obtained by integrating (4.14) from $x > 0$ where $\partial\varphi/\partial x = 0$) when there are $N = 4$ evenly spaced windows. The hood has length $\ell_h = 10R$, and the solid-line curves indicate how the choice $V_0 = 0{\cdot}258$ determined by (4.15) supplies the smoothest variation of $\partial\varphi/\partial x$ at the hood portal, and equal negative peak values for $R\partial^2\varphi/\partial x^2$ at the windows and at the portal.

The corresponding compression and pressure gradient wave profiles for a snub-nosed train (calculated from Equation (4.3) using (4.14)) and normalized as follows

$$p \Big/ \frac{\rho_0 U^2}{(1 - M^2)} \frac{\mathcal{A}_0}{\mathcal{A}} \left(1 + \frac{\mathcal{A}_0}{\mathcal{A}}\right), \qquad \frac{\partial p}{\partial t} \Big/ \frac{\rho_0 U^3}{R(1 - M^2)} \frac{\mathcal{A}_0}{\mathcal{A}} \left(1 + \frac{\mathcal{A}_0}{\mathcal{A}}\right), \tag{4.16}$$

are illustrated in this compact limit in Figure 3 for the two cases of a hood with $N = 4$ and $N = 6$ windows. The approximation to the ideal continuum distribution of windows improves as the number of windows is increased, and the results clearly demonstrate a relatively smaller average pressure gradient and a smoother compression-wave profile when $N = 6$.

5. Noncompact hood

5.1. Stage I approximation

When $\kappa_o\ell_h$ is not negligible, the behaviour of Green's function within the hood must be found from the solution of (3.14) subject to conditions (3.16) and (3.17). To do this, it should first be understood that at this point the window dimensions are already known (and given by (4.11)) in terms of V_0 from the requirement that $\partial\varphi_1(x, 0)/\partial x$ should vary linearly in the compact hood. For evenly spaced windows the value of V_0 is given by (4.15) when the hood is optimal. The investigation of this section will determine the influence on this optimal behaviour of noncompactness, which becomes important at higher train Mach numbers ($M > 0{\cdot}2$).

This means that the conductivities of the windows are known. They will not change when noncompactness becomes important provided that $\kappa_o\ell_x$ and $\kappa_o\ell_\theta$ remain small, *i.e.*, provided

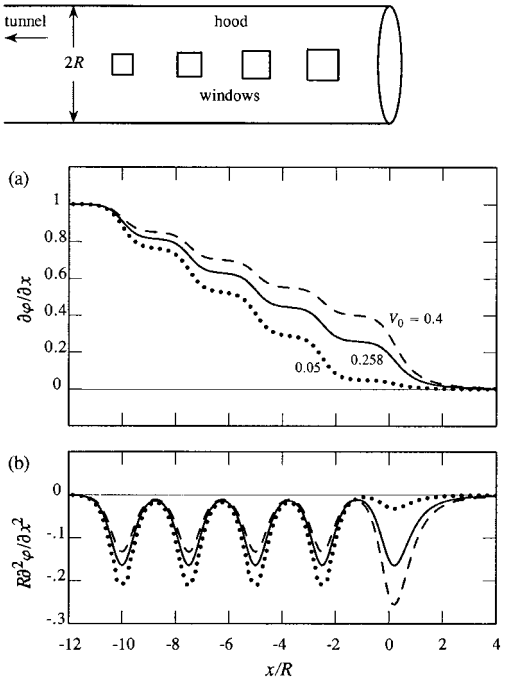

Figure 2. Calculated variations of (a) $\partial\varphi(\mathbf{x}, 0)/\partial x$ and (b) $R\partial^2\varphi(\mathbf{x}, 0)/\partial x^2$ on the hood axis ($r = 0$) for $V_0 = 0{\cdot}05,\ 0{\cdot}258,\ 0{\cdot}4$ in the case of $N = 4$ evenly spaced windows in a hood of length $\ell_h = 10R$. The solid curves are optimal, $V_0 = 0{\cdot}258$ being given by Equation (4.15) to make the negative peak values of $R\partial^2\varphi/\partial x^2$ equal.

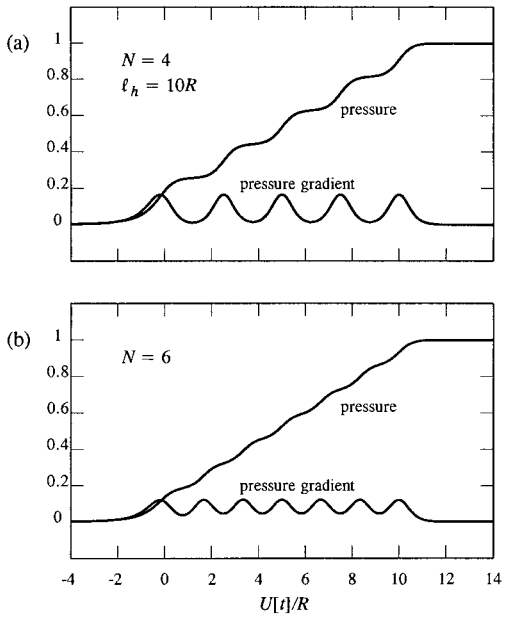

Figure 3. The normalized compression wave and pressure gradient

$$p \Big/ \frac{\rho_0 U^2}{(1-M^2)} \frac{\mathcal{A}_0}{\mathcal{A}} \left(1 + \frac{\mathcal{A}_0}{\mathcal{A}}\right),$$

$$\frac{\partial p}{\partial t} \Big/ \frac{\rho_0 U^3}{R(1-M^2)} \frac{\mathcal{A}_0}{\mathcal{A}} \left(1 + \frac{\mathcal{A}_0}{\mathcal{A}}\right)$$

produced by a snub nosed train entering a hood optimized in the compact limit described in Section 4, for $\ell_h = 10R$ with (a) $N = 4$ and (b) $N = 6$ evenly spaced windows.

that the individual windows are compact, which is certainly the case in practice. The conductivity per unit length of the hood is therefore equal to $-Q(x, 0)/\varphi_1(x, 0)$, so that the sink strength in Equation (3.14) is

$$Q(x, \kappa_o) = \frac{Q(x, 0)\varphi_1(x, \kappa_o)}{\varphi_1(x, 0)}, \tag{5.1}$$

and (3.14) becomes the homogeneous ordinary differential equation

$$\frac{\partial^2 \varphi_1}{\partial x'^2}(x', \kappa_o) + \left(\kappa_o^2 + \frac{Q(x', 0)}{\varphi_1(x', 0)}\right) \varphi_1(x', \kappa_o) = 0, \quad -\ell_h < x' < 0. \tag{5.2}$$

The terms in the large brackets have opposite signs (because $\varphi_1(x, 0)$ is negative within the tunnel and hood), making it evident that the nature of the solution must ultimately change from the hydrodynamic-like behaviour of $\varphi_1(x, 0)$ in a compact hood to a wavelike behaviour as κ_o increases.

Equation (5.2) is to be solved subject to the conditions (3.16) and (3.17). The value of the effective portal exit speed $V \equiv V(\kappa_o)$ is determined by first solving (5.2) as an initial value problem, subject to conditions (3.17) at $x' = 0$ and choosing V to ensure that (3.16) is satisfied at $x' = -\ell_h$. This has to be done numerically, and is facilitated by first setting

$$\varphi_{\rm I}(x', \kappa_o) = V(\kappa_o)\Phi_{\rm I}(x', \kappa_o). \tag{5.3}$$

Then $\Phi_{\rm I}(x', \kappa_o)$ also satisfies (5.2) subject to

$$\Phi_{\rm I}(x', \kappa_o) = -\ell', \quad \frac{\partial \Phi_{\rm I}}{\partial x'}(x', \kappa_o) = 1 \quad \text{at} \quad x' = 0. \tag{5.4}$$

When $\Phi_{\rm I}(x', \kappa_o)$ has been found by numerical integration of (5.2) from $x' = 0$, condition (3.16) yields

$$V(\kappa_o) = \left(\frac{{\rm e}^{-{\rm i}\kappa_o\ell_h}}{\partial\Phi_{\rm I}/\partial x' + {\rm i}\kappa_o\Phi_{\rm I}}\right)_{x'=-\ell_h}, \tag{5.5}$$

and therefore

$$\varphi_{\rm I}(x', \kappa_o) = \frac{\Phi_{\rm I}(x', \kappa_o){\rm e}^{-{\rm i}\kappa_o\ell_h}}{(\partial\Phi_{\rm I}/\partial x' + {\rm i}\kappa_o\Phi_{\rm I})_{x'=-\ell_h}}, \quad -\ell_h < x' < 0. \tag{5.6}$$

5.2. Stage II approximation

When the solution (5.6) has been computed the corresponding source strength $q_n(\kappa_o)$ of the nth window is determined by (3.13), wherein the conductivity K_n is given by (4.11) in general, or by (4.13) for evenly spaced windows.

For N evenly spaced windows we have

$$q_n(\kappa_0) = \frac{-2N\mathcal{A}\Phi_{\rm I}(x_n, \kappa_o){\rm e}^{-{\rm i}\kappa_o\ell_h}}{\Big(n^2\ell_h + 2NV_0(n\ell_h + N\ell')/(1 - V_0)\Big)\Big(\partial\Phi_{\rm I}/\partial x' + {\rm i}\kappa_o\Phi_{\rm I}\Big)_{x'=-\ell_h}}. \tag{5.7}$$

The compression-wave pressure gradient $\partial p/\partial t$ may now be calculated from (3.8), or from (3.11) for the snub-nosed train, by introducing the compressible analogue of (4.8), namely

$$\frac{\partial^2\varphi}{\partial x^2}(\mathbf{x}, \kappa_o) = \sum_{n=1}^{N}\frac{q_n(\kappa_o)}{\mathcal{A}}\frac{\partial^2\varphi_n}{\partial x^2}(r, \theta, x) + V(\kappa_o)\frac{\partial^2\varphi_0}{\partial x^2}(r, \theta, x), \quad r < R. \tag{5.8}$$

To use this formula we define

$$\begin{aligned}\mathcal{F}_n(t) &= \frac{1}{\mathcal{A}}\int_{-\infty}^{\infty} q_n(\kappa_o){\rm e}^{-{\rm i}\omega t}{\rm d}\omega, \quad 1 \le n \le N;\\ \mathcal{F}_0(t) &= \int_{-\infty}^{\infty} V(\kappa_o){\rm e}^{-{\rm i}\omega t}{\rm d}\omega.\end{aligned} \tag{5.9}$$

These functions have the dimensions of time^{-1} and are readily evaluated numerically. Using (5.8) and (5.9) in the representations (3.8) and (3.11), we therefore have, as $x \to -\infty$

$$\frac{\partial p}{\partial t} \approx \frac{-\rho_o U^3}{2\pi(1 - M^2)\mathcal{A}}\left(1 + \frac{\mathcal{A}_{\rm o}}{\mathcal{A}}\right)\sum_{n=0}^{N}\int_{-\infty}^{\infty}\frac{\partial\mathcal{A}_{\rm T}}{\partial x'}(x' + U\tau)\mathcal{F}_n(t - \tau + x/c_o)\frac{\partial^2\varphi_n}{\partial x'^2}(x', 0, 0){\rm d}x'{\rm d}\tau, \tag{5.10}$$

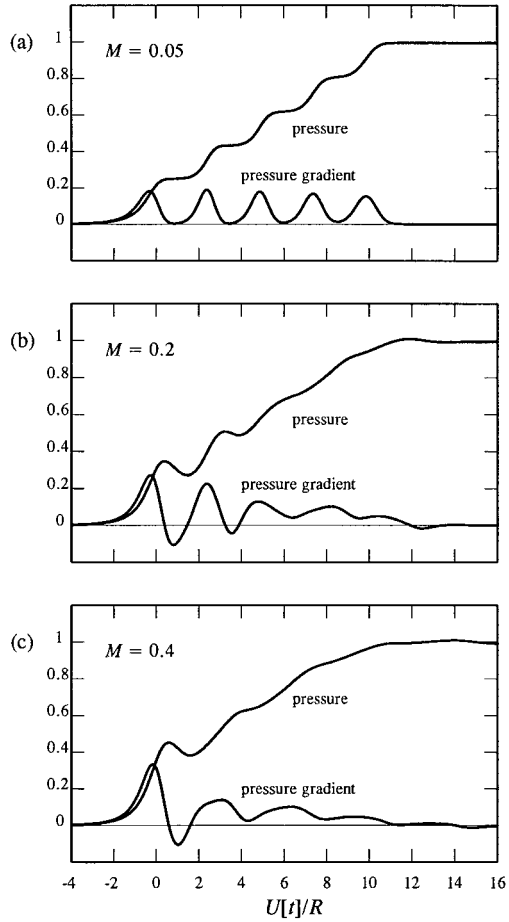

Figure 4. The normalized compression wave and pressure gradient

$$p \Big/ \frac{\rho_0 U^2}{(1-M^2)} \frac{\mathcal{A}_0}{\mathcal{A}} \left(1 + \frac{\mathcal{A}_0}{\mathcal{A}}\right),$$

$$\frac{\partial p}{\partial t} \Big/ \frac{\rho_0 U^3}{R(1-M^2)} \frac{\mathcal{A}_0}{\mathcal{A}} \left(1 + \frac{\mathcal{A}_0}{\mathcal{A}}\right)$$

produced by a snub nosed train entering a hood with $N = 4$ evenly spaced windows, optimized in the compact limit described in Section 4 for $\ell_h = 10R$: (a) $M = 0{\cdot}05$, (b) $M = 0{\cdot}2$ and (c) $M = 0{\cdot}4$.

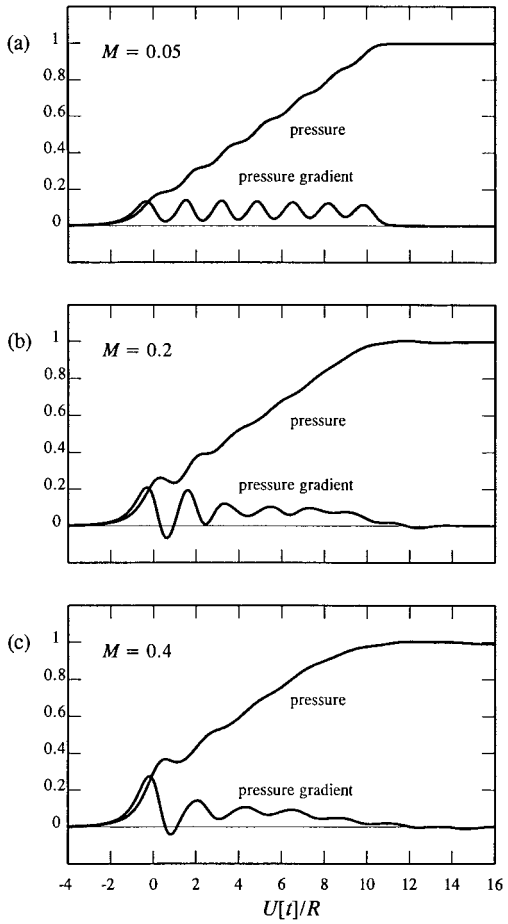

Figure 5. The normalized compression wave and pressure gradient

$$p \Big/ \frac{\rho_0 U^2}{(1-M^2)} \frac{\mathcal{A}_0}{\mathcal{A}} \left(1 + \frac{\mathcal{A}_0}{\mathcal{A}}\right),$$

$$\frac{\partial p}{\partial t} \Big/ \frac{\rho_0 U^3}{R(1-M^2)} \frac{\mathcal{A}_0}{\mathcal{A}} \left(1 + \frac{\mathcal{A}_0}{\mathcal{A}}\right)$$

produced by a snub nosed train entering a hood with $N = 6$ evenly spaced windows, optimized in the compact limit described in Section 4 for $\ell_h = 10R$: (a) $M = 0{\cdot}05$, (b) $M = 0{\cdot}2$ and (c) $M = 0{\cdot}4$.

and for the snub-nosed train

$$\frac{\partial p}{\partial t} \approx \frac{-\rho_o U^3}{2\pi(1-M^2)} \frac{\mathcal{A}_0}{\mathcal{A}} \left(1 + \frac{\mathcal{A}_0}{\mathcal{A}}\right) \sum_{n=0}^{N} \int_{-\infty}^{\infty} \mathcal{F}_n(t - \tau + x/c_o) \frac{\partial^2 \varphi_n}{\partial x'^2}(-U\tau, 0, 0) \mathrm{d}\tau. \qquad (5.11)$$

Figures 4 and 5 depict predictions of the compression wave pressure p and the pressure gradient $\partial p/\partial t$ calculated from (5.11) and normalized as in (4.16) for a snub-nosed train and the three train Mach numbers $M = 0{\cdot}05,\ 0{\cdot}2,\ 0{\cdot}4$. The hood has length $\ell_h = 10R$,

and the figures are, respectively, for the two cases of $N = 4$ and $N = 6$ windows. At the smallest Mach number of $M = 0{\cdot}05$ the plots are indistinguishable from those in Figure 3, computed using the compact hood formula (4.14). As the train speed increases, however, the pressure gradient increases near $U[t]/R = 0$, as the train enters the hood, but is smaller at later times. Thus, it appears that with increased train Mach number the inertia of air within the hood initially resists the entering train causing a sharp but moderate pressure rise which subsequently relaxes as the high-pressure air begins to flow out of the windows. The negative dips in the pressure gradient just after train entry (when $M = 0{\cdot}2,\ 0{\cdot}4$) are probably anomalous predictions (similar to that predicted in [15] for a hood with one window), and would not be observed in practice because such a sharp drop in the pressure gradient is caused by the air flow from the first window, which in practice is impeded by vorticity production in the window, as discussed in detail in [15].

6. Conclusion

There are two principal consequences for compression wave formation of increasing the Mach number of a train entering a tunnel entrance hood fitted with window vents. First, there is an overall increase in the pressure rise across the wave front by a factor

$$\sim \frac{1}{1 - M^2}.$$

This is independent of hood design, and indeed is the same whether or not the tunnel is fitted with a hood, and in a first approximation it has no effect on the *shape* of the wave front profile.

Second, finite Mach number tends to reduce the 'compactness' of the hood length, so that phase differences between the interactions of the train nose with windows at opposite ends of the hood become progressively more important. In the low-Mach-number, compact limit it can be asserted that the whole array of windows distributed along the length of the hood 'work together' to control the compression wave profile. It is then possible to optimize hood performance by adjusting the distribution of the windows and their respective dimensions to ensure that the pressure exhibits the most desirable *linear* growth across the compression wave front for all sufficiently small values of the train Mach number. At high Mach numbers, however, the influences of widely separated windows on the wave are essentially independent; when M exceeds about $0{\cdot}2$ a moderate but significant pressure rise occurs at the head of the wave front at the retarded instant at which the train nose just enters the hood, before the flow in the portal just in front of the nose has had time to adjust to the presence of the more remote hood windows, that render immediate relief for high-pressure air in the compact limit. Once the nose is within the main body of the hood, however, wave-growth becomes substantially smoother and close to linear, as the effective train nose 'sources' find themselves in a relatively homogeneous environment provided by the distributed windows.

The continuum theory described in this paper can be modified in a fairly obvious manner to permit the fine tuning of wave profiles for continuous high speed operations at Mach numbers of, say, $0{\cdot}3$ and higher representative of proposed 'Maglev' services. This will presumably involve a degradation in hood performance at lower Mach numbers, although one can also, perhaps, anticipate the introduction of 'smart' hoods that use speed sensors to automatically adjust window dimensions to optimize hood performance for an entering train.

Acknowledgement

The work reported in this paper is sponsored by the Japan Railway Technical Research Institute administered by Dr. Eng. Tatsuo Maeda. The author gratefully acknowledges the benefit of discussions with Dr. Maeda and with Dr. Masanobu Iida.

References

1. T. Hara, Aerodynamic force acting on a high speed train at tunnel entrance. *Quart. Report Railway Tech. Res. Inst.* 2(2) (1961) 5–11.
2. T. Hara, M. Kawaguti, G. Fukuchi and A. Yamamoto, Aerodynamics of high-speed train. *Monthly Bull. Int. Railway Congr. Assoc.*, XLV(2) (1968) 121–146.
3. S. Ozawa, Y. Morito, T. Maeda and M. Kinosita, Investigation of the pressure wave radiated from a tunnel exit. *Railway Tech. Res. Inst. Report* 1023 (1976) (in Japanese); Railway Technical Research Institute, 2-8-38 Hikari-cho, Kokubunji-shi, Tokyo 185-8540.
4. W. A. Woods and C. W. Pope, Secondary aerodynamic effects in rail tunnels during vehicle entry. In: H. S. Stephens, R. R. Dowden, A. L. King and M. P. Patel (eds.), *Second BHRA Symposium of the Aerodynamics and Ventilation of Vehicle Tunnels*. Cambridge, England (23–25 March 1976) pp. 71–86.
5. S. Ozawa and T. Maeda, Model experiment on reduction of micro-pressure wave radiated from tunnel exit. In: R. I. Emori (ed.), *Proceedings of the International Symposium on Scale Modeling*, Seikei University, Japan Society of Mechanical Engineers. Tokyo (18–22 July 1988) pp. 33–37.
6. S. Ozawa, T. Maeda, T. Matsumura, K. Uchida, H. Kajiyama and K. Tanemoto, Countermeasures to reduce micro-pressure waves radiating from exits of Shinkansen tunnels. In: A. Haerter (ed.), *Aerodynamics and Ventilation of Vehicle Tunnels*. Elsevier Science Publishers (1991) pp. 253–266.
7. M. Schultz and H. Sockel, Pressure transients in railway tunnels. In: W. Schneider, H. Troger and F. Ziegler (eds.), *Trends in Applications of Mathematics to Mechanics*. Harlow: Longman (1991) pp. 33–39.
8. T. Maeda, T. Matsumura, M. Iida, K. Nakatani and K. Uchida, Effect of shape of train nose on compression wave generated by train entering tunnel. In: M. Iguchi (ed.), *Proceedings of the International Conference on Speedup Technology for Railway and Maglev Vehicles*. Yokohama, Japan, 22-26 November, Tokyo University (1993) pp. 315–319.
9. M. Iida, T. Matsumura, K. Nakatani, T. Fukuda and T. Maeda, Optimum nose shape for reducing tunnel sonic boom. *Institution of Mechanical Engineers* Paper C514/015/96 (1996).
10. T. Maeda, Private communication (2000).
11. M. S. Howe, On the design of a tunnel-entrance hood with multiple windows. *Boston University Report* AM-02-001, January 2002; submitted for publication in the *J. Sound Vibr.*
12. M. S. Howe, M. Iida, T. Fukuda and T. Maeda, Theoretical and experimental investigation of the compression wave generated by a train entering a tunnel with a flared portal. *J. Fluid Mech.* 425 (2000) 111–132.
13. M. S. Howe, The compression wave produced by a high-speed train entering a tunnel. *Proc. R. Soc. London* A454 (1998) 1523–1534.
14. M. S. Howe, Mach number dependence of the compression wave generated by a high-speed train entering a tunnel. *J. Sound Vibr.* 212 (1998) 23–36.
15. M. S. Howe, M. Iida, T. Fukuda and T. Maeda, Aeroacoustics of a tunnel-entrance hood with a rectangular window. Submitted to *J. Fluid Mech.* (August, 2002).
16. B. Noble, *Methods Based on the Wiener-Hopf Technique*. London: Pergamon Press (1958; reprinted 1988 by Chelsea Publishing Company, New York.) 246 pp.
17. M. S. Howe, The compression wave generated by a high-speed train at a vented tunnel entrance. *J. Acoust. Soc. Am.* 104 (1998) 1158–1164.
18. M. S. Howe, Prolongation of the rise time of the compression wave generated by a high speed train entering a tunnel. *Proc. Roy. Soc. London* A455 (1999) 863–878.
19. Lord Rayleigh, *The Theory of Sound*, Volume 2. London: Macmillan (1926).
20. M. Abramowitz and I. A. Stegun (eds.), *Handbook of Mathematical Functions* (Ninth corrected printing), US Department of Commerce, National Bureau of Standards Applied Mathematics Series No.55 (1970).